Global embedding of the Kerr black hole event horizon into hyperbolic 3-space

G. W. Gibbons,[1,*] C. A. R. Herdeiro,[2,†] and C. Rebelo[2,‡]

[1]*D.A.M.T.P., Cambridge University, Wilberforce Road, Cambridge CB3 0WA, U.K.*
[2]*Departamento de Física e Centro de Física do Porto, Faculdade de Ciências da Universidade do Porto, Rua do Campo Alegre, 687, 4169-007 Porto, Portugal*

An explicit global and unique isometric embedding into hyperbolic 3-space, H^3, of an axi-symmetric 2-surface with Gaussian curvature bounded below is given. In particular, this allows the embedding into H^3 of surfaces of revolution having negative, but finite, Gaussian curvature at smooth fixed points of the $U(1)$ isometry. As an example, we exhibit the global embedding of the Kerr-Newman event horizon into H^3, for arbitrary values of the angular momentum. For this example, considering a quotient of H^3 by the Picard group, we show that the hyperbolic embedding fits in a fundamental domain of the group up to a slightly larger value of the angular momentum than the limit for which a global embedding into Euclidean 3-space is possible. An embedding of the double-Kerr event horizon is also presented, as an example of an embedding that cannot be made global.

I. INTRODUCTION

Since Gauss proved his famous *theorema egregium*, it has become customary to make a clear distinction between the intrinsic properties of a closed surface S, whether local quantities such as its Gauss curvature

$$K = \frac{1}{R_1 R_2}, \tag{1}$$

where R_1, R_2 are the principal radii of curvature,

or nonlocal quantities such as its area A, which depend only on the metric, and extrinsic properties such as its mean curvature

$$H = \frac{1}{2}\left(\frac{1}{R_1} + \frac{1}{R_2}\right), \tag{2}$$

which is local, or its largest diameter D, which is nonlocal, since these may depend on which particular embedding one adopts.

However, this distinction may break down if the embedding in question is *rigid*, that is unique. By theorems of Weyl, Pogorelov, and others (see [1,2]), this is true of smooth 2-surfaces whose Gauss curvature is everywhere positive; then there exists, up to isometries, a unique isometric embedding into Euclidean 3-space $\mathbb{E}^3$. Since this embedding $\mathbf{x} = \mathbf{x}(u^i)$ is given by three highly nonlinear partial differential equations depending on the intrinsic metric,

$$g_{ij} = \partial_i \mathbf{x}. \partial_j \mathbf{x}, \tag{3}$$

the extrinsic quantities depend in a highly nonlocal fashion on the metric.

---
*G.W.Gibbons@damtp.cam.ac.uk
†crherdei@fc.up.pt
‡mrebelo@fc.up.pt

If the Gauss curvature is somewhere negative, then S may or may not admit a global isometric embedding into $\mathbb{E}^3$. In [3] an example of a 2-surface with a patch of negative curvature that can be globally embedded into $\mathbb{E}^3$ is given (another simple example is a "donut"-like surface); in the same reference it is also shown that if the 2-surface admits a $U(1)$ action and the Gaussian curvature is negative at a smooth fixed point of such action, then a vicinity of the fixed point cannot be embedded, not even locally, into $\mathbb{E}^3$. If the fixed point having negative Gaussian curvature is not smooth, however, a global embedding may exist. An example is the Kerr ergosphere [4], on a constant Boyer-Lindquist time slice [5].

But if the Gauss curvature is bounded below by some negative constant,

$$K \geq -\frac{1}{L^2}, \tag{4}$$

then Pogorelov [6] has shown that there is always an isometric embedding, unique up to isometries, into hyperbolic space H^3 with radius of curvature L. By scaling L may always be taken to be unity.

These facts have clear relevance to general relativity, both at the classical and the quantum level:

(i) Historically (e.g. [7–10]; see also [11]), isometric embeddings have frequently been used to gain intuition about geometric features of spacetimes. If the embedding is rigid, then such intuition is less likely to be misleading than if the embedding is flexible, and many equivalent embeddings exist. For an interesting account of flexible nonconvex polyhedra see [12].

(ii) In recent efforts to define a so-called quasilocal mass [13], functional associated with a two surface S, embedded in a four-dimensional Lorentzian spacetime, use has been made of the Pogorolev

theorem to embed S isometrically into H^3 and hence considering H^3 as points equidistant to the future from some origin (i.e. the mass shell) in flat Minkowski spacetime $\mathbb{E}^{3,1}$. The embedding into $\mathbb{E}^{3,1}$ is not expected to be unique.

(iii) In a recent paper [14], one of us gave an intrinsic formulation of Thorne's Hoop conjecture, and used as a technical tool an isometric embedding into $\mathbb{E}^3$ to prove it in some particular cases.

In this paper, we shall, with these motivations in mind, provide explicit isometric embeddings of the horizons of Kerr-Newman and double Kerr-Newman black holes into H^3. The former is global. The latter is local, because of the presence of a strut, which is required to keep the two black holes apart.

An isometric embedding of the Kerr-Newman horizon into $\mathbb{E}^3$ was first given by Smarr [8] who discovered that for $J > \sqrt{3}M^2/2$ the Gauss curvature K at the North and South poles becomes negative, and a global isometric embedding into $\mathbb{E}^3$ is no longer possible. A local embedding into three-dimensional Minkowski spacetime $\mathbb{E}^{2,1}$ is possible but this is not global [15]. To circumvent this problem Frolov [3] has given a global embedding into four-dimensional Euclidean space $\mathbb{E}^4$. It is not known whether the Frolov embedding is rigid, but it seems unlikely.

II. THE UPPER HALF SPACE MODEL

Events (T, X, Y, Z) in $\mathbb{E}^{3,1}$ are in one-to-one correspondence with Hermitian two by two matrices

$$\mathbf{X} = \begin{pmatrix} T + Z & X + iY \\ X - iY & T - Z \end{pmatrix}, \qquad (5)$$

and the Lorentz group $SO(3, 1) = PSL(2, \mathbb{C})$ acts as

$$\mathbf{X} \to S\mathbf{X}S^\dagger, \qquad \mathbf{X} \in SL(2, \mathbb{C}). \qquad (6)$$

Translations act as matrix addition

$$X \to X + A. \qquad (7)$$

Hyperbolic space H^3 corresponds to events

$$\mathbf{X} = \begin{pmatrix} \frac{1}{z} & \frac{x+iy}{z} \\ \frac{x-iy}{z} & \frac{x^2+y^2}{z} + z \end{pmatrix}, \qquad z > 0, \qquad x + iy \in \mathbb{C}. \qquad (8)$$

To embed H^3 into Minkowski spacetime $\mathbb{E}^{3,1}$ one simply equates the two matrix formulas above. The induced metric on the surface

$$X^2 + Y^2 + Z^2 - T^2 = -1 \qquad (9)$$

is then

$$ds^2 = \frac{1}{z^2}(dz^2 + dx^2 + dy^2). \qquad (10)$$

It is now simple to embed any surface in the upper half space model of H^3 (10) into $\mathbb{E}^{3,1}$.

III. IDENTIFICATIONS

Rather than embedding into H^3, one might consider making identifications under the action of some discrete subgroup $\Gamma \subset SO(3, 1)$. Quotients H^3/Γ, which are closed or possibly merely of finite volume, are of interest in cosmology, in models where the spatial sections of $k = -1$ Friedman-Lemaitre universes are taken to be of the so-called non-Euclidean honeycomb form H^3/Γ [16]; they are also of interest in some Kaluza-Klein compactifications [17,18]. The simplest noncompact quotient of finite volume is obtained by taking Γ to be the Picard group [19] $SL(2, \mathbb{G})$, where $\mathbb{G}$ are the Gaussian integers $m + in$, m, $n \in \mathbb{Z}$. This is a double quotient $SL(2, \mathbb{G})\backslash SL(2, \mathbb{C})/SU(2)$. This example has been used in cosmology for studies of the effects of global spatial topology on the cosmic microwave background [20,21].

A fundamental domain, completely analogous to the fundamental domain of the modular group $SL(2, \mathbb{Z})$, acting on the upper half plane is [19]

$$|x| \leq \tfrac{1}{2}, \qquad |y| \leq \tfrac{1}{2}, \qquad x^2 + y^2 + z^2 \geq 1. \qquad (11)$$

Below we shall exhibit the embedding of the Kerr-Newman event horizon into H^3 and show that up to a certain value of the angular momentum it can be taken to lie completely inside this fundamental domain.

There is an interesting connection with the unique four-dimensional self-dual Lorentzian lattice $\Pi^{3,1}$ [22]. The mathematics and physics literatures differ somewhat in their use of the word lattice. In the mathematical literature a *lattice* Λ is taken to be a finitely generated discrete Abelian group. Thinking of Λ as a subgroup of $\mathbb{R}^n$ leads us to the toroidal quotient $T^n = (S^1)^n = \mathbb{R}^n/\Lambda$. In the present case one may think of the lattice as matrices A in (7) whose entries are Gaussian integers. In the physics literature a *lattice* is usually taken to be a set of points in $\mathbb{R}^n$ invariant under the action of a lattice Λ. Typically these points are the orbits in $\mathbb{R}^n$ of a lattice Λ. A further source of confusion is that the underlying affine space $\mathbb{R}^n$, is frequently endowed with a metric of signature (s, t). Thus, the mathematicians at least, should speak of a lattice with metric, especially since the theory of the classification of such lattices depends crucially on the signature of the metric.

In the present case $(s, t) = (3, 1)$, corresponding to restricting (T, X, Y, Z) to take integer values [22]. The point group of the lattice is $SO(3, 1; \mathbb{Z})$ [16], which is covered by Picard's group $SL(2, \mathbb{G})$. The corresponding lattice, in the physical sense, was used by Schild in an attempt to model a discrete spacetime [23,24]. One can also think of the associated quotient as a spacetime that is periodic both in space and in time. An interesting question is then whether one may embed our surfaces into a unit cell of this lattice universe, which we shall address in the example of Sec. V.

IV. GENERAL EMBEDDING FORMULAE

We shall now present the explicit embedding formulas for a 2-surface admitting a $U(1)$ action in H^3. We start with the upper half space model for hyperbolic 3-space H^3, discussed in Sec. II:

$$ds^2 = \frac{L^2}{z^2}(dx^2 + dy^2 + dz^2) = \frac{L^2}{z^2}(dr^2 + r^2 d\phi^2 + dz^2),$$

$$(12)$$

where L is the "radius" of the hyperbolic space, $z > 0$ and in the last equality we have used polar coordinates. We wish to construct a global embedding of the 2-surface

$$ds^2 = R^2(a^2(u)du^2 + b^2(u)d\phi^2) \qquad (13)$$

in H^3. The functions $a(u)$, $b(u)$ are dimensionless; u is a polar coordinate with range $-1 \leq u \leq 1$, with equalities attained, respectively, at the South and North poles; R is a length scale. The embedding functions are

$$r(u) = \frac{b(u)z(u)}{k},$$

$$(b(u)^2 + k^2)\frac{z'(u)}{z(u)} = -b(u)b'(u)$$

$$\pm \sqrt{[a(u)b(u)]^2 + k^2[a(u)^2 - b'(u)^2]},$$

$$(14)$$

where $k = L/R$. To make contact with the embedding used in [8] for the Kerr-Newman horizon and in [25] for the double-Kerr horizons we take $a(u)^2 = 1/b(u)^2 = 1/g(u)$; then, the embedding functions are

$$r(u) = \frac{\sqrt{g(u)}z(u)}{k},$$

$$(g(u) + k^2)\frac{z'(u)}{z(u)} = -\frac{g'(u)}{2} \pm \sqrt{1 + \frac{k^2}{g(u)}\left[1 - \frac{g'(u)^2}{4}\right]}.$$

$$(15)$$

In limit of large radius k (i.e. flat space limit) these functions reduce to

$$\tilde{r}(u) = R\sqrt{g(u)}, \qquad \tilde{z}'(u) = \pm\sqrt{\frac{R^2}{g(u)}\left[1 - \frac{g'(u)^2}{4}\right]},$$

$$(16)$$

where $\tilde{r}$ and $\tilde{z}$ are cylindrical polar coordinates in $\mathbb{E}^3$. These are exactly the embedding functions used in [25]. Thus, while the embedding in $\mathbb{E}^3$ will fail when $g'(u)^2 > 4$, the same embedding in H^3 will be possible if $g'(u)$ is bounded. The advantage of using hyperbolic space becomes therefore manifest. Note that the Gaussian curvature of the 2-surface is

$$K = -\frac{g''(u)}{2R^2}. \qquad (17)$$

From this formula one can see that the failure of the embedding is not directly associated to the Gaussian curvature becoming negative. This is manifest in the Kerr-Newman example—see Fig. 1.

V. THE KERR-NEWMAN HORIZON

As a first application of the general formulae of Sec. IV let us consider the Kerr-Newman event horizon. In this case [8],
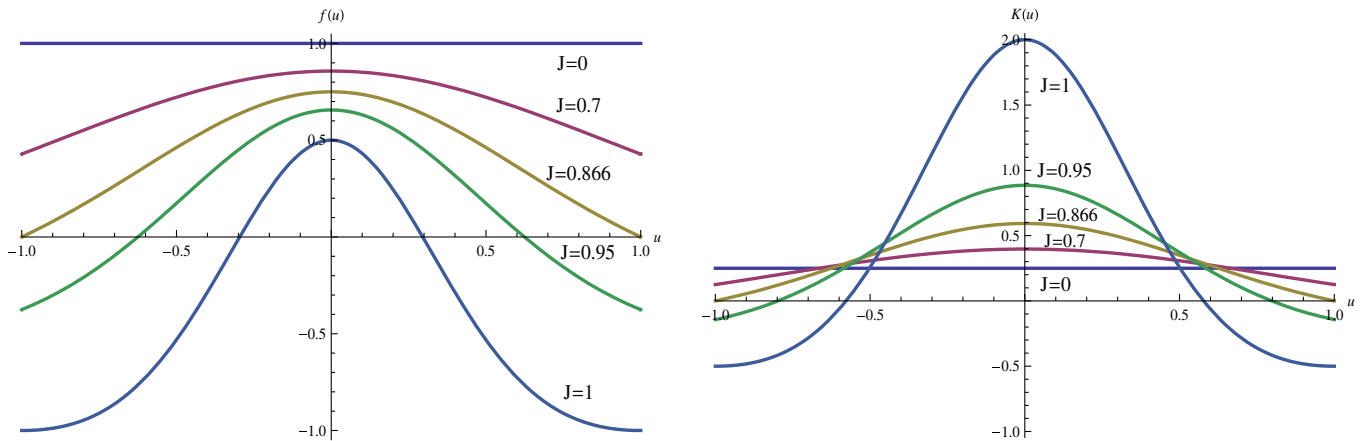

FIG. 1 (color online). $f(u)$ (left) and Gauss curvature (right) for the Kerr-Newman solution, for fixed mass $M = 1$ and various values of the angular momentum J. The embedding in $\mathbb{E}^3$ fails when the $f(u)$ becomes negative; this function is bounded by -1 for any J. Note that there are regions where the curvature is positive but the embedding fails.
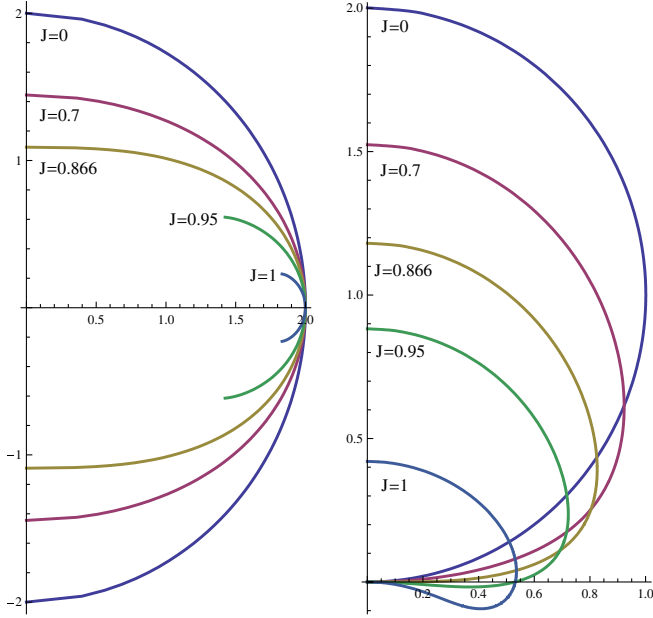
FIG. 2 (color online). Profile of the embedding in $\mathbb{E}^3$ (left, first presented in [25]) and H^3 (right, using $k = 1$) of the Kerr horizon, for fixed mass $M = 1$ and various values of the angular momentum J. For the hyperbolic embedding only the shape is relevant, not the overall scaling, since the latter depends on an arbitrary integration constant.

$$g(u) = \frac{(1 - u^2)(1 + c^2)}{1 + c^2 u^2},$$

$$c \equiv \frac{J}{M(M + \sqrt{M^2 - J^2/M^2})},$$

$$R^2 = 2M\left(M + \sqrt{M^2 - \frac{J^2}{M^2}}\right), \qquad (18)$$

where M, J are the Arnowitt-Deser-Misner mass and angular momentum of the black hole. Note that $0 \leq c \leq 1$ for black hole solutions, with the equalities attained for Schwarzschild and extreme Kerr, respectively. The embedding in flat space will fail when the function

$$f(u) \equiv (1 - g'(u)^2/4)/g(u) \qquad (19)$$

becomes negative. This function is plotted in Fig. 1. The figure shows that, for $J > \sqrt{3}/2$, the embedding in $\mathbb{E}^3$ fails in two patches around each of the poles (two polar caps). The function $f(u)$ is bounded from below, and has a minimum given by $f = -1$. Therefore, to embed the complete surface in H^3 it suffices to take $L = R$, i.e. $k = 1$. In Fig. 2 the profiles of the embeddings in $\mathbb{E}^3$ and H^3, $z = z(r)$ are displayed. In the latter case, the overall scaling is irrelevant, since it is determined by an arbitrary integration constant.

Surprisingly, the embedding of the round sphere (the $J = 0$ case) in $\mathbb{E}^3$ and H^3 are identical. The hyperbolic embedding of the round sphere can be treated analytically. From (15) one gets

$$(\ln z)' = \frac{u \pm \sqrt{1 + k^2}}{1 + k^2 - u^2}. \qquad (20)$$

The two solutions are interchanged by the reparameterization $u \to -u$. Integrating yields

$$z = \frac{\alpha}{\sqrt{1 + k^2} - u}, \qquad \alpha = \text{constant} > 0. \qquad (21)$$

Using (15), one arrives at the surface equation

$$r^2 + \left(z - \frac{\alpha\sqrt{1 + k^2}}{k^2}\right)^2 = \frac{\alpha^2}{k^4}. \qquad (22)$$

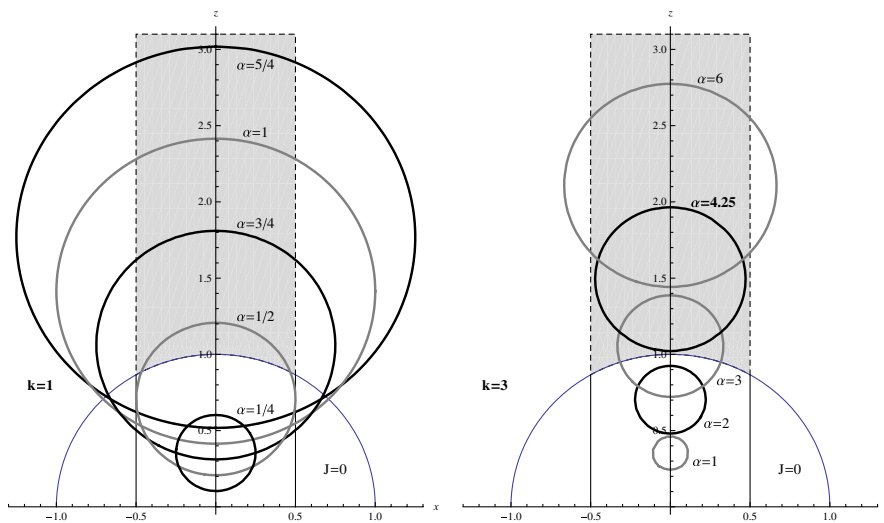This is indeed the standard equation of a spherical surface

FIG. 3 (color online). Embedding the round 2-sphere ($J = 0$) into H^3 for $k = 1$ (left) and $k = 3$ (right) and various values of α. For $k = 1$ ($k = 3$) the embedding cannot (can, taking an appropriate α) be fitted completely inside the fundamental domain (11)—shaded region. We display the x, z plane—as in Fig. 4, 7, and 8—but note that the embedded surface has a $U(1)$ isometry in the $x - y$ plane.
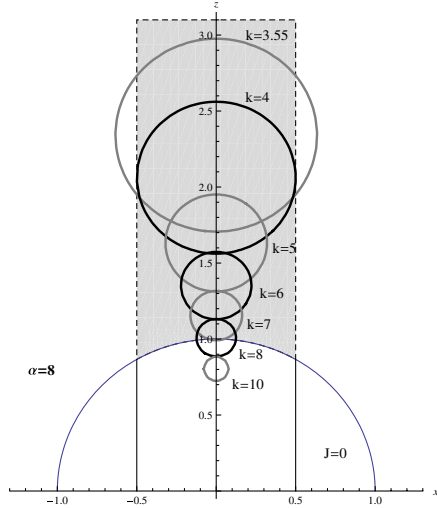
FIG. 4 (color online). Embedding the round 2-sphere ($J = 0$) into H^3 for $\alpha = 8$ and various values of k. The embedding can, taking the value of k in an appropriate range, be fitted completely inside the fundamental domain (11)—shaded region.

(but note that these are the coordinates of the upper half space model for H^3). In Fig. 2 we have taken $k = 1 = \alpha$ and we have performed a z translation so that the plot intersects the origin.

Observe that the embedding of the round sphere can be fitted in the fundamental domain discussed in Sec. III. Indeed, if suffices to take k, α such that $\alpha/k^2 < 1/2$ and $(\sqrt{1 + k^2} - 1)\alpha/k^2 > 1$. This is possible if k is sufficiently large and choosing the value of α appropriately—Fig. 3; in

this figure the effect of increasing α for constant k can be seen: it raises the center of the sphere and increases its radius. The same effect is obtained, for constant α, *decreasing* the value of k—Fig. 4.

We can use the embedding of H^3 in four-dimensional Minkowski space given in Sec. II to check that (22) describes a round sphere. Noting that $r^2/z^2 = X^2 + Y^2$ and $z = 1/(T + Z)$, we find the surface

$$X^2 + Y^2 + \left(\frac{\alpha}{k}(T + Z) - \frac{\sqrt{1 + k^2}}{k}\right)^2 = \frac{1}{k^2}. \qquad (23)$$

The 2-surface described by (22) is the intersection of (23) with H^3 embedded in $\mathbb{E}^{3,1}$ as the surface (9). This yields the codimension two set in $\mathbb{E}^{3,1}$ described by

$$X^2 + Y^2 + \left(\sqrt{1 - v^2}Z + \frac{v\sqrt{1 + k^2}}{k}\right)^2 = \frac{1}{k^2},$$

$$\frac{1}{\sqrt{1 - v^2}}(T + vZ) = \frac{\sqrt{1 + k^2}}{k}, \qquad (24)$$

where the "velocity" v is defined as

$$v \equiv \frac{\alpha^2 - k^2}{\alpha^2 + k^2}. \qquad (25)$$

Introducing "boosted" coordinates

$$T' = \frac{1}{\sqrt{1 - v^2}}(T + vZ), \qquad Z' = \frac{1}{\sqrt{1 - v^2}}(Z + vT), \qquad (26)$$

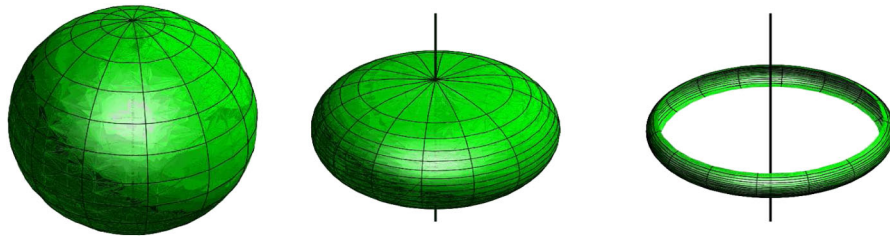(9) becomes $X^2 + Y^2 + Z'^2 - T'^2 = -1$ and the 2-surface

FIG. 5 (color online). Embedding the Kerr horizon for fixed mass $M = 1$ and various values of the angular momentum J ($J = 0$, 0.86, 1) in $\mathbb{R}^3$. In the extremal case the embedding covers only a region of the horizon around the equator [8].
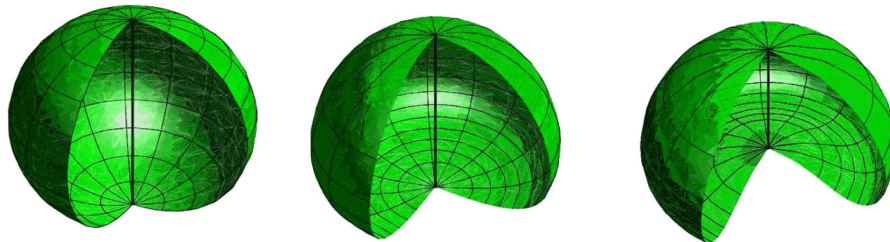

FIG. 6 (color online). Embedding the Kerr horizon for fixed mass $M = 1$ and various values of the angular momentum J ($J = 0$, 0.86, 1) in H^3, with $k = 1$. The embedding covers the whole of the horizon, even in the extremal case. Note, however, that the $\mathbb{Z}_2$ symmetry around the equator is lost, when the angular momentum is turned on. This is to be expected, since it is not a symmetry of the embedding space. But surprisingly the symmetry remains in the $J = 0$ case.
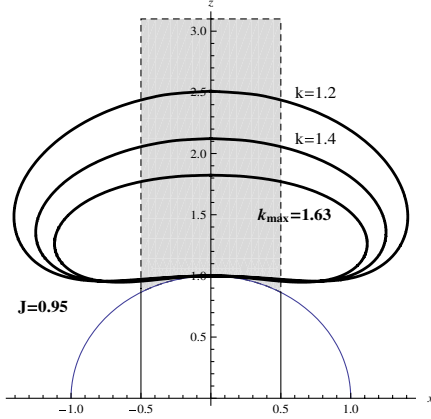
FIG. 7 (color online). Embedding the Kerr-Newman event horizon for $M = 1$ and $J = 0.95$ into H^3 for various values of k and of an additional integration constant α, fixed at $\alpha = \alpha_{touch}$. No choice can fit the embedding completely inside the fundamental domain (11) [shaded region].

(24) becomes

$$X^2 + Y^2 + Z'^2 = \frac{1}{k^2}, \qquad T' = \frac{\sqrt{1 + k^2}}{k} > 1. \qquad (27)$$

This is indeed a round 2-sphere; the apparent ellipsoid exhibited in (24) is a result of Lorentz contraction.

In Figs. 5 and 6 we present 3D plots of the embeddings of the Kerr-Newman event horizon in $\mathbb{E}^3$ and H^3, respectively, for various values of the angular momentum. In the hyperbolic case the embedding is global for any value of J.

Note that in the Euclidean case, even a local embedding of the region around the poles is impossible for $J > \sqrt{3}/2$ [3].

For $J \neq 0$ it is still possible to fit the embedding completely inside the fundamental domain, but only up to a maximal value of J/M^2, which is in [0.8725, 0.8735]. This interval has been determined numerically with the following strategy. First observe that, fixing the black hole, i.e. J and M, the embedding depends on k and on an additional integration constant α, as in the $J = 0$ case treated above analytically. Fixing k, the effect of increasing α is to move the embedding profile up in the z coordinate, making it simultaneously larger, as in the $J = 0$ case (cf. Fig. 3). Thus, our strategy is

(i) for each k, α is fixed at $\alpha = \alpha_{touch}$, such that the points in the embedding profile with the smallest z touch tangentially the boundary of the fundamental domain at $r^2 + z^2 = 1$;

(ii) analyzing different values of k, each with $\alpha = \alpha_{touch}$, one realizes that the effect of decreasing k is to increase the size of the profile—see Fig. 7 for an example.

(iii) since k is bounded above for $J/M^2 = \sqrt{3}/2$ we investigate, beyond this value of the angular momentum, the embedding profile for the maximum allowed $k = k_{max}$ and $\alpha = \alpha_{touch}$.

It turns out that for values of J/M^2 slightly above $\sqrt{3}/2 \simeq 0.866$ (we checked up to 0.8725) it is still possible to fit the embedding in the fundamental domain; but for $J/M^2 = 0.8735$ this is not the case anymore—Fig. 8.
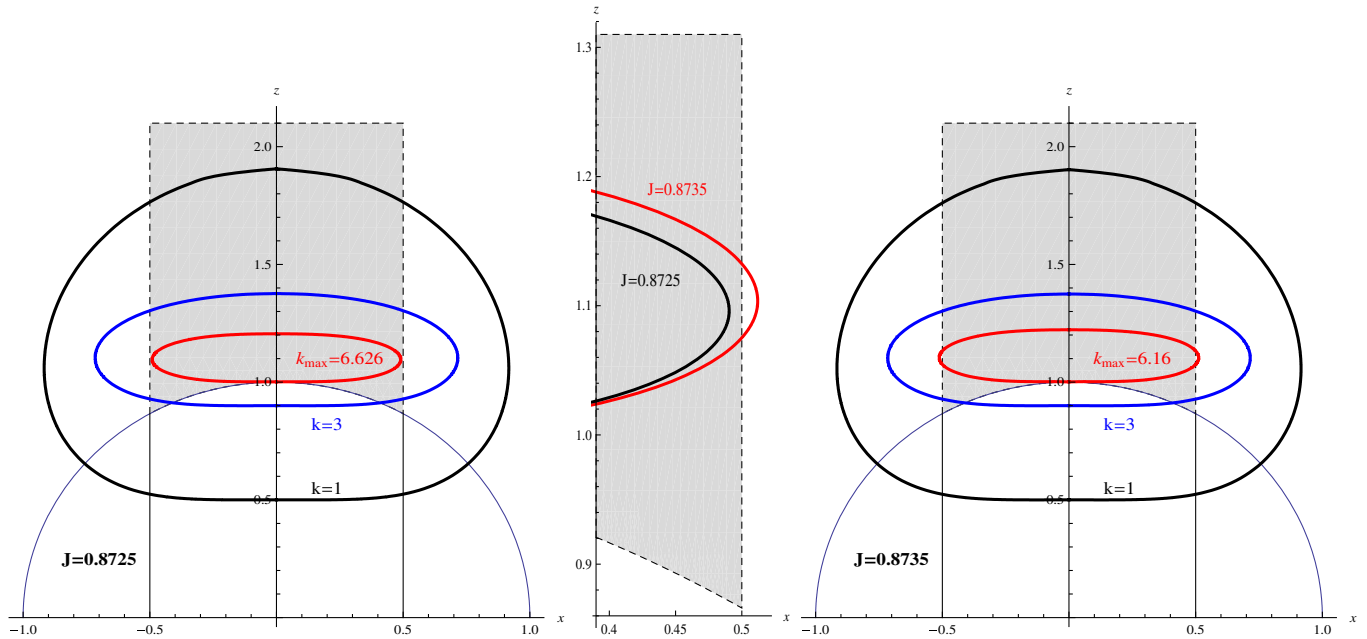

FIG. 8 (color online). Embedding the Kerr-Newman event horizon for $M = 1$, $J = 0.8725$ (left) and $J = 0.8735$ (right) into H^3 for various values of k, including for each case k_{max} and $\alpha = \alpha_{touch}$. In the former case the embedding can still be fitted inside the fundamental domain (11) (shaded region), but not in the latter case, which is explicit in the detail (middle).

VI. THE DOUBLE-KERR HORIZON

As a second example we shall now consider the embedding of the double-Kerr event horizon. The double-Kerr solution is a 7-parameter vacuum spacetime. It was originally generated using a Bäcklund transformation [26]. But it can also be generated using the inverse scattering technique [27]. The general solution is extremely complex. But two 3-parameter subfamilies have been recently analyzed. These are the counter-rotating [27] and corotating case [25]. These two families describe two stationary coaxial Kerr black holes, with the same mass and the same (corotating) or opposite (counter-rotating) angular momentum. They are asymptotically flat and they obey the "axis condition," which guarantees that the azimuthal Killing vector field has zero norm on the symmetry axis. The three parameters of the solutions are, therefore, the mass of each black hole ($M_1 = M_2 \equiv M$), their angular momentum ($J_1 = \pm J_2 \equiv J$), and the distance between them ζ. The latter parameter is the coordinate distance in Weyl canonical coordinates. But it is a measure of the proper distance d, in the sense that the latter is a monotonic function of ζ [25].

The asymptotically flat double-Kerr solution for two black holes always has a strut. Physically, this strut provides the necessary force to keep the two black holes in equilibrium. Mathematically it is described by a conical singularity with a conical excess.

In [25], the embedding of the double-Kerr horizon was performed in $\mathbb{E}^3$. We shall now perform it in H^3. The first observation is that, unlike the Kerr horizon, the embedding in hyperbolic space is not global. The reason can be appreciated in Figs. 9 and 10, where we have plotted the function $f(u)$, for the counter-rotating case, for various values of ζ and J, fixing $M = 1$ and choosing the "lower" black hole in the double-Kerr system, i.e. the one with the strut on its North pole ($u = 1$). It can be seen that the
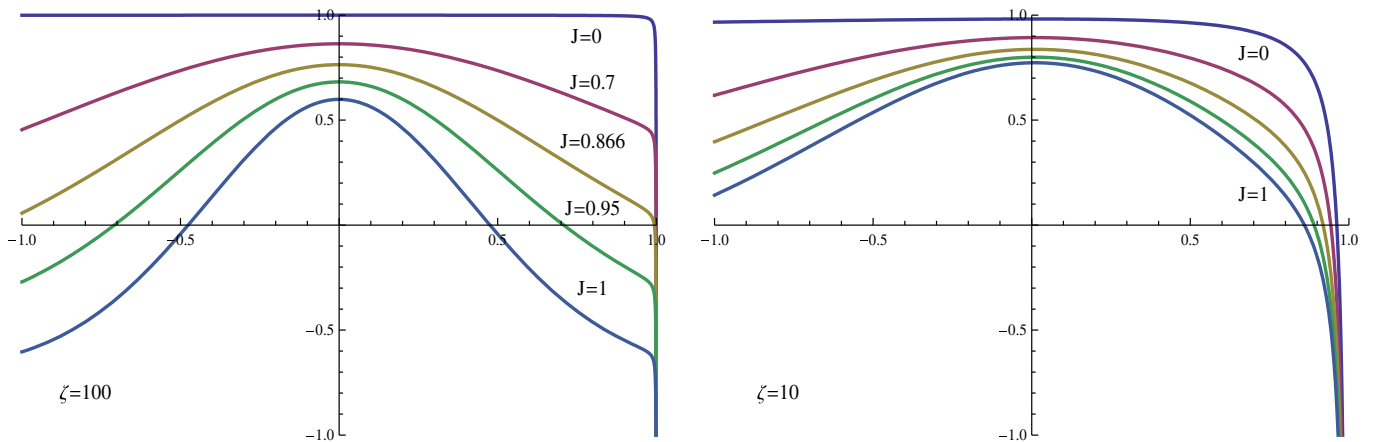

FIG. 9 (color online). Function $f(u)$ for $\zeta = 100$ (left) and $\zeta = 10$ (right), fixed mass $M = 1$ and various values of the angular momentum J. The left plot corresponds to a large distance and therefore resembles Fig. 1 (i.e. the case of an isolated black hole), except at the North pole ($u = 1$), where the strut meets the horizon.
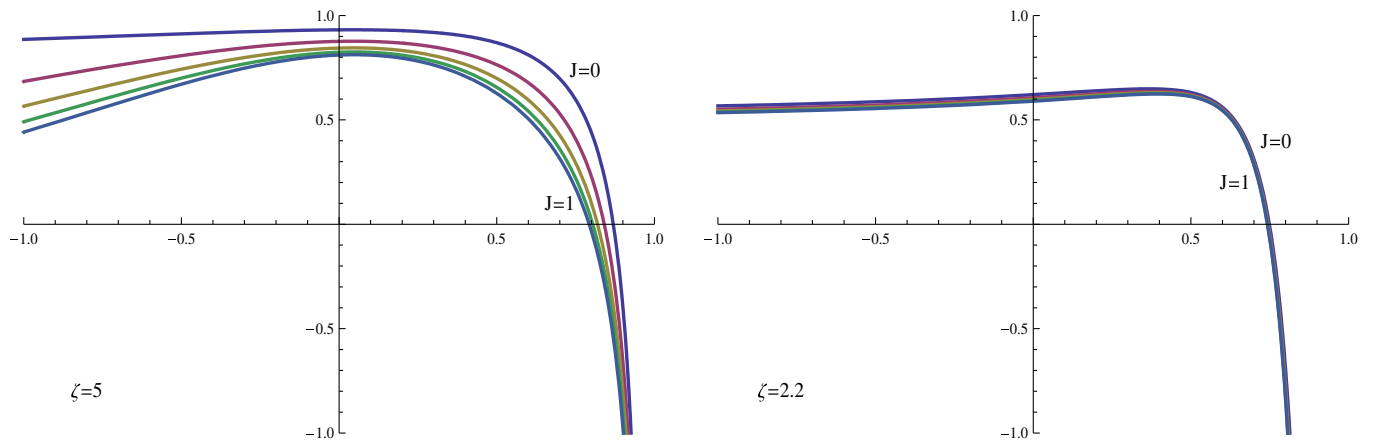

FIG. 10 (color online). Function $f(u)$ for $\zeta = 5$ (left) and $\zeta = 2.2$ (right), fixed mass $M = 1$ and various values of the angular momentum J. As the distance decreases, the function becomes less sensitive to the angular momentum, and approaches that of a nonrotating black hole, albeit deformed near the North pole.
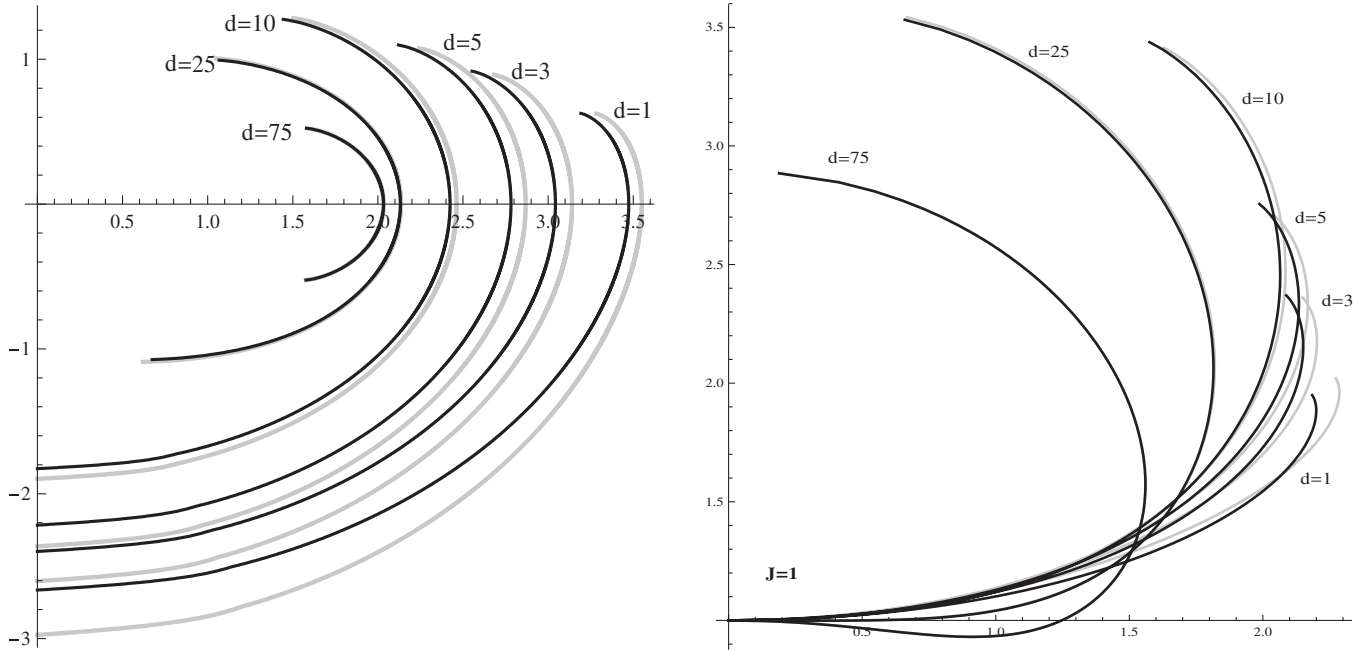
FIG. 11.   Profile of the embedding in $\mathbb{E}^3$ (left, first presented in [25]) and H^3 (right, using $k = 1$) of the double-Kerr horizon, for fixed mass and angular momentum $M = 1 = J$ and various values of the *physical* distance in between the two black holes. At the north pole there is a "strut," and the embedding always fails. The grey (black) lines correspond to the counter-rotating (corotating) case.

function $f(u)$ always diverges at $u = 1$. This is to be expected and corresponds to the location of the strut. Thus, irrespectively of the value of k, the embedding will never completely cover the surface.

Figure 9 shows that the behavior of $f(u)$ is very similar in the double-Kerr system and in the single Kerr system for large distance ($\zeta = 100$). There is however, a difference in behavior at the North pole, where the strut meets the horizon. As the distance between the two black holes decreases, the function $f(u)$ approaches that of a nonrotating black hole, albeit somewhat deformed, cf. Figs. 9 and 10. This was interpreted in [27] as being caused by the mutual rotational dragging slow down that the black holes exert on one another.

One may ask how much of the horizon surface is covered by the hyperbolic embedding, fixing a value of k. Somewhat surprisingly, choosing the minimal value of k that covers the whole surface in the limit of infinite distance ($k = 1$) and for two black holes with $|J| = M^2$, the hyperbolic embedding does not appear to cover more of the horizon surface than the Euclidean one, for small distances—Fig. 11.

In Figs. 12 and 13 we present 3D plots of the embeddings in $\mathbb{E}^3$ and H^3 of the lower black hole in the counter-rotating double-Kerr system.
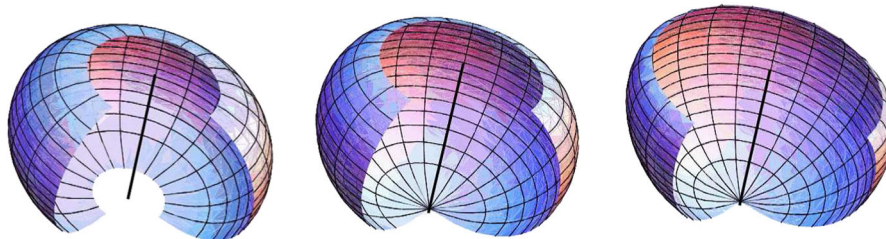

FIG. 12 (color online).   Embedding the lower black hole in double-Kerr horizon for fixed mass and angular momentum $M = 1 = J$ and various values of the physical distance d ($d = 25, 10, 3$) in $\mathbb{E}^3$. As the distance decreases: i) the South pole gets covered by the embedding (this is a consequence of the smaller angular velocity of the black hole); ii) there is a growing patch around the North pole that is not covered by the embedding, manifesting the deformation induced by the strut, which becomes stronger as the interaction between the two black holes becomes stronger.
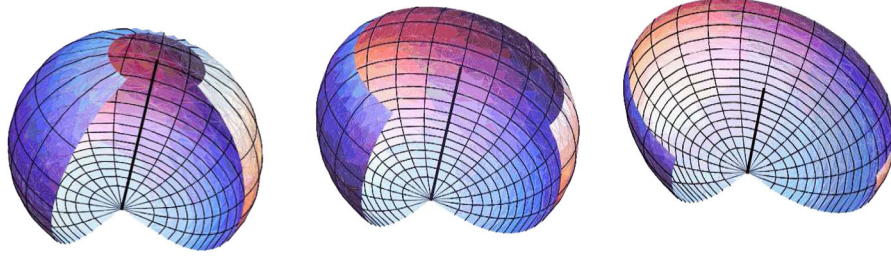
FIG. 13 (color online).   Embedding the double-Kerr horizon for fixed mass and angular momentum $M = 1 = J$ and various values of the physical distance d ($d = 25, 10, 3$) in H^3, with $k = 1$. Unlike the Euclidean embedding, the South pole is always covered by the hyperbolic embedding. As in the Euclidean embedding, there is a growing patch around the North pole that is not covered by the hyperbolic embedding, manifesting the deformation induced by the strut. The patch does not appear smaller than in the Euclidean embedding.

VII. CONCLUSIONS AND FINAL REMARKS

In this paper we have discussed global and unique isometric embeddings of 2-surfaces in hyperbolic 3-space. Such embeddings are possible as long as the Gaussian curvature of the 2-surface is bounded below. As an example we considered the embedding for the Kerr-Newman black hole event horizon. According to a fundamental theorem of Riemannian geometry [28], every smooth n-dimensional Riemannian manifold can be globally isometrically embedded in an N-dimensional Euclidean space, where $N = (n + 2)(n + 3)/2$.[1] For $n = 2$ this yields $N = 10$. An embedding in a lower dimensional space may, nevertheless, be possible. Indeed, it was shown by Frolov that for the Kerr-Newman case, a global embedding in $\mathbb{E}^4$ is possible. Herein, we have shown that a global and unique embedding in a three-dimensional *hyperbolic* space is possible for all values of the angular momentum, in contrast with the embedding in Euclidean 3-space, first described in [8], which is only global for $J/M^2 \leq \sqrt{3}/2$. Moreover, we have shown that up to $J/M^2 \simeq 0.873 > \sqrt{3}/2$, the hyperbolic embedding can be fitted in a fundamental domain of the Picard group, which is used to construct interesting quotients of hyperbolic space.

Recently, various physical properties of the double-Kerr system were studied [25,27]. One novel feature unveiled in these studies is that the angular velocity of the two black holes decreases as they are approached, keeping their mass and angular momentum fixed, for both the counter-rotating [27] and corotating [25] cases. This effect was interpreted as a consequence of the mutual rotational dragging of the black holes. The angular velocity decrease is visible in the horizon geometry, and therefore in its embedding in a higher dimensional space. Although the effect of the angular velocity decrease is clearer in the Euclidean embedding, it is also visible in the hyperbolic embedding exhibited herein. Because of the existence of a strut that provides the force balance between the black holes, there is a curvature singularity at one of the poles of the horizon and therefore the embedding (both Euclidean and hyperbolic) is not global.

Other possible applications of the hyperbolic embedding are to Kerr-(anti) de Sitter black holes and to a Schwarzschild black hole immersed in a magnetic field. In the latter case it has been shown [31] that a patch of negative Gaussian curvature develops, near the equator, if the magnetic field parameter exceeds a certain limit. Curiously, for a certain range of magnetic field values, the Gaussian curvature of a Kerr black hole immersed in a magnetic field becomes positive for all values of the angular momentum, and an embedding in $\mathbb{E}^3$ is possible [32].

---

[1]A *local* embedding, is possible in a lower dimensional Euclidean space, $\mathbb{E}^N$, with $N = n(n + 1)/2$, according to a theorem first proved by Janet for 2-manifolds [29] and subsequently generalised by Cartan for n-dimensional manifolds [30]. Note that the dimension of the embedding space is the number of components of the metric tensor of the manifold.

[1] H. Hopf, *Differential Geometry in the Large*, Lecture Notes in Mathematics Vol. 1000 (Springer-Verlag, Berlin, 1989).

[2] L. Nirenberg, in *Non-Linear Problems*, edited by R. E. Langer (University of Wisconsin, Madison, 1963).

[3] V. P. Frolov, Phys. Rev. D **73**, 064021 (2006).

[4] N. Pelavas, N. Neary, and K. Lake, Classical Quantum Gravity **18**, 1319 (2001).

[5] T. Jacobson and Y. A. Soong, Classical Quantum Gravity **26**, 055014 (2009).

[6] A. V. Pogorelov, Adv. Math. **1**, 191 (1965).

[7] L. Flamm, Phys. Z. **17**, 448 (1916), in particular, p. 450.

[8] L. Smarr, Phys. Rev. D **7**, 289 (1973).

[9] A. Friedman, Rev. Mod. Phys. **37**, 201 (1965).

[10] J. Rosen, Rev. Mod. Phys. **37**, 204 (1965).

[11] H. Goenner, in *General Relativity and Gravitation: One Hundred Years after the Birth of Einstein*, edited by A. Held (Plenum Press, New York, 1980), Vol. 1.

[12] I. Stewart, Sci. Am. **July** 90 (1998).

[13] M.-T. Wang and S.-T. Yau, arXiv:0805.1370.

[14] G. W. Gibbons, arXiv:0903.1580.

[15] G. W. Gibbons, C. A. R. Herdeiro, C. M. Warnick, and M. C. Werner, Phys. Rev. D **79**, 044022 (2009).

[16] H. S. M. Coxeter and G. J. Whitrow, Proc. R. Soc. A **201**, 417 (1950).

[17] M. Gell-Mann and B. Zwiebach, Nucl. Phys. **B260**, 569 (1985).

[18] A. A. Bytsenko and M. E. X. Guimares, Proc. Sci. WC2004 (2004) 017.

[19] M. E. Picard, Bull. Math. Soc. France **12**, 43 (1884).

[20] B. Aurich, S. Lustig, F. Steiner, and H. Then, Classical Quantum Gravity **21**, 4901 (2004).

[21] B. Aurich, S. Lustig, F. Steiner, and H. Then, Phys. Rev. Lett. **94**, 021301 (2005).

[22] P. Goddard and D. Olive, in *Workshop on Vertex Operators in Mathematics and Physics, Berkeley, California* (Report No. DAMTP-83/22, 1983).

[23] A. Schild, Phys. Rev. **73**, 414 (1948).

[24] A. Schild, Can. J. Math. **1**, 29 (1949).

[25] M. S. Costa, C. A. R. Herdeiro, and C. Rebelo, Phys. Rev. D **79**, 123508 (2009).

[26] G. Neugebauer and D. Kramer, Phys. Lett. A **75**, 259 (1980).

[27] C. A. R. Herdeiro and C. Rebelo, J. High Energy Phys. 10 (2008) 017.

[28] J. Nash, Annals of Math. **63**, 20 (1956).

[29] M. Janet, Ann. Soc. Polon. Math. **5**, 38 (1926).

[30] E. Cartan, Ann. Soc. Polon. Math. **6**, 1 (1927).

[31] W. J. Wild and R. M. Kerns, Phys. Rev. D **21**, 332 (1980).

[32] R. Kulkarni and N. Dadhich, Phys. Rev. D **33**, 2780 (1986).